Effect of operating depth on the optimal lugged wheel design for hand tractors in paddy fields

Taufik Rizaldi*, Indra Saputra Kurniawan, Robert Sinaga

(Study Program of Agricultural and Biosystem Engineering, Universitas Sumatera Utara, Medan 20155, Indonesia)

Abstract: The performance of agricultural machinery, particularly hand tractors, in paddy fields is highly influenced by soil conditions. This study focuses on determining the optimal design parameters for lugged wheels to enhance the traction and efficiency of paddy-field operations. The analysis was conducted at three soil operating depths (5, 10, and 15 cm) to evaluate the performance of the lugged wheels. Key design parameters, including the wheel diameter, number of lugs, and lug width, length, and angle, were optimised based on the vertical force (*Fv*), horizontal force (*Fh*), and torque measurements. The results revealed that the optimal wheel design for 5- and 10-cm depths was similar, featuring eight lugs with a 77-cm diameter, 7-cm lug width, 28-cm lug length, and 20° lug angle. However, the performance metrics varied, with *Fv*, *Fh*, and torque values of 138.97 kg, 152.04 kg, and 508.87 N m at 5 cm, respectively, compared to 155.51 kg, 170.83 kg, and 571.82 N m at 10 cm, respectively. For a 15-cm depth, the optimal design required nine lugs, with *Fv*, *Fh*, and torque values of 291.56 kg, 350.12 kg, and 1175.14 N m, respectively. These findings provide critical insights into the optimisation of lugged-wheel designs for improving traction and efficiency in paddy fields. This study highlights the importance of considering the soil depth when designing wheels for agricultural machinery, offering a practical framework for enhancing the performance of hand tractors in challenging field conditions.

Keywords: optimization, design parameters, vertical force, horizontal force, torque performance

Citation: Rizaldi, T., I. S. Kurniawan, and R. Sinaga. 2026. Effect of operating depth on the optimal lugged wheel design for hand tractors in paddy fields. Agricultural Engineering International: CIGR Journal, 28(1):84-93.

1 Introduction

Advancement of agricultural mechanisation has become a key focus in enhancing productivity and efficiency, particularly in paddy fields, which have a significantly higher water content than dry land. However, the soft and water-saturated soil in paddy fields poses considerable challenges for tractor mobility, often leading to inefficiency and equipment damage. Consequently, improving tractor movement in paddy fields is essential, particularly through the optimisation of wheel designs as the primary propulsion system (Pentoś and Pieczarka, 2017). Lugged wheels have become an important solution for improving traction in soft terrains, such as wet farmland and planetary surfaces. Research by Chen et al. (2020) and Bao et al. (2020) showed that wheel designs with lugs can reduce slip by up to 15%–20% compared to conventional wheels, especially in muddy soil conditions. The principle of work is simple but effective: the lugs serve as an additional "grip" that increases the frictional force between the wheel and soil.

The development of lugged wheels must consider complex wheel-soil interactions. A study by Du et al. (2017) using the discrete element method (DEM)

Received date: 2025-02-24 **Accepted date:** 2025-05-21

***Corresponding author: Taufik Rizaldi.** Study Program of Agricultural and Biosystem Engineering, Universitas Sumatera Utara, Medan, Indonesia. Email: taufik.rizaldi@usu.ac.id.

revealed that the performance of lugs is significantly influenced by their geometry (height, width, and angle) and distribution pattern. The simulation results showed that lugs with a height of 50–70 mm and a distance between lugs of 1.5–2 times the height of the lugs provides optimal traction while minimising rolling resistance. These findings are consistent with those of Md-Tahir et al. (2023) for agricultural tractors.

The application of lugged wheels in extreme environments, such as planetary exploration, poses new challenges. Jayalekshmi and Gireesh Kumar (2019) found that in lunar simulation soil (TRI-1), lugged wheels experienced a 30% lower sinkage than plain wheels. However, Wang et al. (2020) cautioned that an overly aggressive design could increase the risk of wheel slip in sandy terrain. Innovative solutions, such as position-adjustable active lugs (Yang et al., 2018) and adaptive suspension systems (Gao et al., 2024), have been developed to address this issue.

In the agricultural sector, lugged wheel optimisation is performed to balance traction and environmental impact. Delmond et al. (2024) warned that an improper lug design can lead to excessive soil compaction. Zhou et al. (2017) recommended a combination of shorter lugs (30 mm–40 mm) with more even wheel pressure. This approach has been proven to reduce soil compaction by up to 25%, while maintaining traction performance.

Nevertheless, the application of lugged wheels in paddy fields often results in soil depression because of the force required to generate sufficient activation power. This underscores the importance of soil strength in achieving effective traction. This phenomenon is linked to traction generation as a reaction of the drive wheel against the soil, which largely depends on soil conditions and quality. It has been further confirmed that traction results from the interaction between the propulsion force generated by the wheels, tracks, and other relevant equipment with the soil. Understanding variations in lugged wheel design parameters, such as the angle, spacing, size, shape, mechanism, and circumferential angle, is crucial for optimising tractor performance in paddy fields (Kim et al., 2020).

Research on the design and optimisation of lugged wheels has been pivotal for enhancing the traction performance across diverse terrain conditions, especially in agricultural and off-road applications. Further investigation by Fajardo and Suministrado (2019) who analyzed the effects of lug angle, shaft speed, and number of passes on the puddling characteristics of tilling wheels and revealed that optimal configurations can enhance soil preparation efficiency. Additionally, computational modelling approaches have expanded the understanding of wheel-terrain interactions, as demonstrated by Aoshima et al. (2021) and Agarwal et al. (2019), who developed simulation-based models for optimising high-performance wheel loading and granular media interactions, respectively. The integration of advanced modelling techniques, such as real-time wheel detection and rim classification by Staněk et al. (2023) and the development of an instrumented wheel-on-limb system for planetary rovers by Feng et al. (2022), highlights the evolving complexity and interdisciplinary nature of lugged wheel research. These innovations not only enhance the understanding of lug mechanics, but also pave the way for adaptable wheel designs that can respond to varying environmental challenges.

Recently, advanced technologies have been increasingly integrated into the design of lugged wheels. Kim and Cho (2023) successfully developed a deep-learning-based slip ratio estimation system that increased the prediction accuracy by up to 92%. Salazar Luces et al. (2020) introduced wheels with variable lug lengths that can be automatically adjusted to different types of terrain. These innovations provide new opportunities for the development of more efficient and adaptive lugged wheels.

Collectively, these studies emphasise the significance of lug design in optimising traction, minimising soil disturbance, and improving vehicle efficiency in challenging environments. As technology advances, the integration of computational models and real-time monitoring systems continues to refine

lugged-wheel functionality, fostering improvements in agricultural productivity, off-road mobility, and exploratory missions. Based on these findings, it is evident that lugged wheel design should not only focus on improving traction, but also consider factors such as energy efficiency, material durability, and environmental impact.

2 Material and methods

Soil penetration resistance measurements were carried out in Lengau Seprang Village, Tanjung Morawa District, Deli Serdang Regency, North Sumatra, using a penetrometer proving ring whose ends were mounted with plates measuring 5 × 5 cm^2, 5 × 10 cm^2, 5 × 15 cm^2 and 5 × 20 cm^2 alternately with varying pressure angles ranging from 30°, 45°, 60°, 75° and 90° at depths of 5, 10 and 15 cm from the soil surface. Measurements were made by adjusting the dynamic movement of the wheel lugs when they entered the soil during operation. The lugged wheel designed for paddy fields was based on the construction factors of the tractor, the strength of the soil, and the soil movement pattern.

The measurement of paddy fields directly in the study location were sandy clay, with a sand, dust, and clay contents of 51%, 24%, and 25%, respectively was measured as dry base are presented in the following Table 1.

Meanwhile, the tractor data used to determine wheel design parameters is presented in the following Table 2.

Table 1 Experimental site moisture content and bulk density

Soil depth level (cm)	Moisture content (%)	Bulk density (g cm^{-3})
5	136.43	0.61
10	129.15	0.63
15	113.8	0.71

Table 2 Yanmar Type Tf85 Mly-Di tractor data

Parameter	Data
Total weight (*Wt*)	273.3 kg
Soil clearance (*Hc*)	≥ 5 cm
Sinkage (*Z*)	≤ 20 cm
Basic radius of the gearbox (*Ht*)	11.5 cm
Crank arm distance to the wheel shaft	49 cm
Plough width	20 cm
Plough depth	20 cm
Plough specific draft	0.25 kg cm^{-2}
Rolling resistance coefficient	0.2

2.1 Wheel diameter

The design of the lugged wheel diameter requires a focus on the space available for the wheels on the tractor to be used. This is to ensure that the body of the tractor does not touch the soil level at the time of operation, as indicated in Figure 1 (Rizaldi and Sumono, 2020).

Therefore, the soil clearance (H_c), which is the distance between the soil level and the body of the hand tractor, must be considered. The minimum size of the outer radius of the wheel R_w (cm) was determined using Equation 1.

$$R_w = H_t + H_c + Z \quad (1)$$

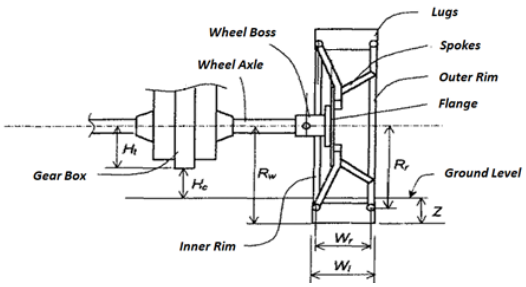

Figure 1 Scheme for determining the wheel design parameters

where, H_t is the radius of the gearbox (cm), H_c is the soil clearance (cm), and Z is sinkage (cm) (Rizaldi and Sumono, 2020).

2.2 Number of lugs

The lugged wheels used in paddy fields have wider and fewer lugs than those applied to dry lands. A wider distance between the lugs, longer pitch, or smaller

number of lugs significantly reduce the occurrence of chunks of soil sticking or becoming trapped between the lugs. Moreover, the reaction force of the soil on the lugs is affected by the distance or space between the lugs. This occurs because the closeness of the lugs to each other reduces the concentration of soil and vice versa, as indicated in Figure 2 (Rizaldi and Sumono, 2020).

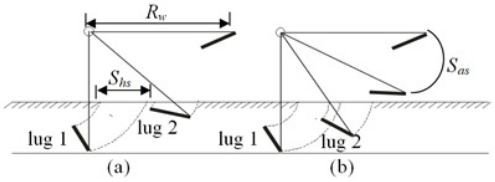

(a) lug 8 (b) lug 12

Figure 2 Lug-focused soil on both lug 8 and lug 12

The distance was determined using the following equations developed by Rizaldi and Sumono (2020):

$$S_{as} = 2R_w \sin\left[\frac{360^o}{J_s}\right] \quad (2)$$

$$S_{hs} = \frac{(1-S)\pi D_w}{J_s} \quad (3)$$

Where,

S_{as} is the distance between the lugs (cm);

J_s is the number of lugs;

S_{hs} is the horizontal distance between the lugs (cm);

S is the wheel slip (%);

D_w is the outer diameter of the wheel (cm).

2.3 Lugs angle

The angle between the lugs was determined to ensure that good vertical and horizontal forces were exerted during the soil movement. This is based on the condition that the surface of the lugs should be exactly at the soil level, as shown in Figure 3 (Rizaldi and Sumono, 2020).

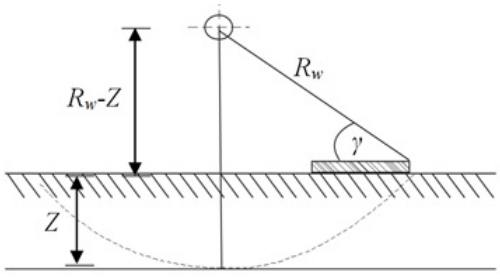

Figure 3 Position of the plate above the soil level

The information in Figure 3 was used to determine the lug angle (γ) as follows:

$$\sin\gamma = \frac{R_w - Z}{R_w} \text{ n} \quad (4)$$

$$\gamma = \sin^{-1}\left(\frac{R_w - Z}{R_w}\right) \quad (5)$$

Where,

γ is the angle of the lugs (°);

R_w is the outer radius of the wheel (cm);

Z is the sinkage (cm) (Rizaldi and Sumono, 2020).

2.4 Number of active lugs

Active lugs were defined as lugs entering the soil during operation. The number of active lugs typically indicates the amount of lift, thrust, and torque generated by the wheel. Therefore, the system presented in Figure 4 was used to determine this information (Rizaldi and Sumono, 2020).

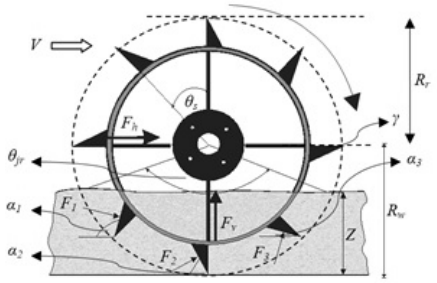

Figure 4 Illustration of a wheel system acting on the soil surface

The figure shows that the number of active lugs working on the soil surface can be calculated using the following equations (Rizaldi and Sumono, 2020):

$$\theta_{jr} = 2\cos^{-1}\left[\frac{(R_w - Z)}{R_w}\right] \quad (6)$$

$$R_r = \frac{D_w}{2} - L_s\cos\gamma \quad (7)$$

$$J_{sa} = \frac{\theta_{jr}}{360} J_s \quad (8)$$

where F is the force generated by the lugs of the wheel (kg), F_v is the vertical force of the wheel (kg), F_h is the horizontal force of the wheel (kg), θ_s is the angel between the lugs (°), θ_{jr} is the angle formed by the intersection of the soil surface and the rim of the wheel (°), D_w is the outer diameter of the wheel (cm), R_w is the outer radius of the wheel (cm), R_r is the rim radius (cm), Z is the sinkage (cm), L_s is the lug width

(cm), J_{sa} is the number of active lugs, and J_s is the number of lugs.

2.5 Sinkage

The sinkage of each active lug was calculated using the following formula based on the number of odd and even lugs as follows (Rizaldi and Sumono, 2020).

For an odd number of the lugs:

$$Z_n = Z \tag{9}$$

$$Z_{n-1} = Z_{n+1} = Z - \left[\left(\frac{D_r}{2}\right)(1-\cos\theta_s)\right]$$

$$Z_{n-2} = Z_{n+2} = Z - \left[\left(\frac{D_r}{2}\right)(1-\cos 2\theta_s)\right]$$

$$Z_{n-3} = Z_{n+3} = Z - \left[\left(\frac{D_r}{2}\right)(1-\cos 3\theta_s)\right]$$

For an even number of the lugs:

$$Z_{n-1} = Z_{n+1} = Z - \left[\left(\frac{D_r}{2}\right)(1-\cos(\frac{\theta_s}{2})\right] \tag{10}$$

$$Z_{n-2} = Z_{n+2} = Z - \left[\left(\frac{D_r}{2}\right)(1-\cos(\theta_s+\frac{\theta_s}{2})\right]$$

$$Z_{n-3} = Z_{n+3} = Z - \left[\left(\frac{D_r}{2}\right)(1-\cos(2\theta_s+\frac{\theta_s}{2})\right]$$

where D_r is the diameter of the rim (cm).

2.6 Forces acting on the lugs

The forces acting on the lugs (F_r, F_v, and F_h) and the rolling resistance force (F_{rr}) were determined using Equations 11–14, as indicated in Figure 5 (Rizaldi and Sumono, 2020).

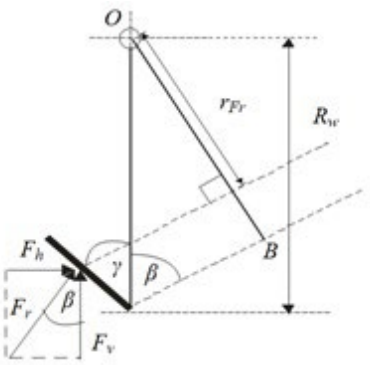

Figure 5 Soil reaction force diagram for torque determination

Figure 5 shows the dynamic movement of the lugs as they enter the soil. The lugs press on the soil, while the soil exerts a reaction force involving both vertical and horizontal forces, and this system is defined in the following equations (Rizaldi and Sumono, 2020).

$$F_r = \sum_{j=1}^{i=j_{sa}} A_s.P_i \tag{11}$$

$$F_v = F_r \cos\beta \tag{12}$$

$$F_h = F_r \sin\beta \tag{13}$$

$$F_r = \sqrt{F_h^{\,2} + F_v^{\,2}} \tag{14}$$

$$\beta = \tan^{-1}\left(\frac{F_h}{F_v}\right) \tag{15}$$

$$OB = R_w \times \sin\beta \tag{16}$$

$$r_{Fr} = OB - \left(\frac{L_s}{2}\right) \tag{17}$$

Where,

A_s is the area of the lugs (cm^2);

P_i is the pressure of soil penetration (Pa);

F_r is the resultant force (kg);

β is the angle (°) formed by the resultant and vertical forces;

r_{Fr} is the arm of F_r, (cm) ;

L_s is the width of the lugs (cm).

Analysis was conducted to determine the design parameters of the lugged wheel on the hand tractor. The total reaction force (T_r) generated by the lugs was evaluated based on the soil strength (Rizaldi and Sumono, 2020).

$$T_r = F_r \times r_{Fr} \tag{18}$$

$$T_r = F_r \times \left\{\left(R_w \times \sin\beta\right) - \left(\frac{L_s \cos(\gamma+\beta-90)}{2}\right)\right\} \tag{19}$$

The soil penetration value was determined by directly measuring the depth and angle of suppression based on suppression plates of several sizes in the paddy fields. The accumulated force must overcome the weight of the tractor as well as the wheel rolling resistance to ensure traction (Rizaldi and Sumono, 2020).

$$F_v \geq 0.5W_t \tag{20}$$

$$F_d = DSP \times l \times d \tag{21}$$

$$F_{rr} = W_t \times C_{rr} \tag{22}$$

$$F_h \geq 0.5\left(F_d + F_{rr}\right) \quad (23)$$

where W_t is the weight of the tractor (kg), F_d is the drawbar force (kg), DSP is the specific draft of the plough (kg cm^{-2}), l is the width of the plough (cm), d is the depth of the plough (cm), F_{rr} is the force (kg) required to adjust the resistance of the rolling wheel, and C_{rr} is the rolling resistance coefficient.

3 Results and discussion

The soil penetration resistance measurement results for each plate size, the depth of emphasis and the angle of emphasis are highly dependent on the physical properties of the soil (Tables 3-6) .

Table 3 Experimental site soil penetration resistance data against 5 × 5 cm^2 plates

Sinkage (cm)	*P* (kPa)				
	Angle 90°	Angle 75°	Angle 60°	Angle 45°	Angle 30°
5	65.739	46.141	23.958	6.096	4.012
10	144.017	75.963	42.939	20.563	25.501
15	199.571	124.650	63.039	62.267	42.592

Table 4 Experimental site soil penetration resistance data against 5 × 10 cm^2 plates

Sinkage (cm)	*P* (kPa)				
	Angle 90°	Angle 75°	Angle 60°	Angle 45°	Angle 30°
5	51.503	6.906	7.870	25.347	24.228
10	100.113	60.685	33.911	55.901	47.221
15	178.931	108.331	74.960	73.301	58.988

Table 5 Experimental site soil penetration resistance data against 5 × 15 cm^2 plates

Sinkage (cm)	*P* (kPa)				
	Angle 90°	Angle 75°	Angle 60°	Angle 45°	Angle 30°
5	66.434	41.473	37.924	27.931	26.080
10	166.431	116.510	108.987	99.805	85.415
15	282.285	248.644	135.877	135.028	122.721

Table 6 Experimental site soil penetration resistance data against 5 × 20 cm^2 plates

Sinkage (cm)	*P* (kPa)				
	Angle 90°	Angle 75°	Angle 60°	Angle 45°	Angle 30°
5	142.628	59.296	43.402	9.413	8.950
10	193.977	170.752	143.978	101.425	93.748
15	343.588	293.010	193.784	165.158	150.382

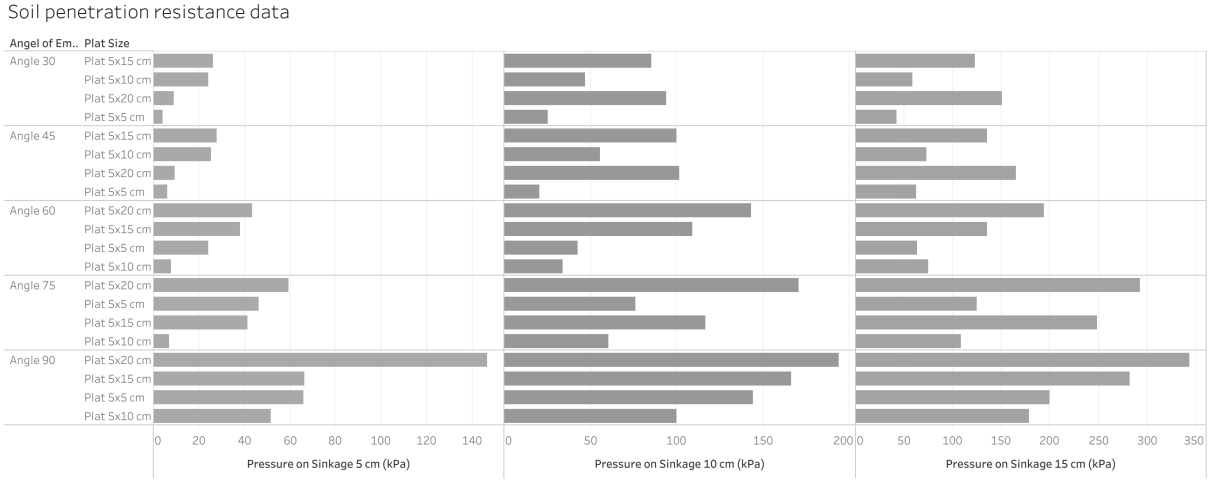

Figure 6 Effect of pressure depth, pressure angle and plat size on soil penetration resistance

The design parameters of the analysed lugged wheel included the diameter of the wheel and number, size, and angle of the lugs. These parameters were determined based on the soil penetration resistance value for each depth as well as the angle of emphasis of the particular plate generated through direct measurements. The deeper the plate enters the soil, the greater the compressive force because a greater depth corresponds to harder rice field soil owing to soil compaction. In addition, a larger plate size results in a greater compressive force. However, the pressure on the soil in such a system is smaller because the pressure is inversely proportional to the plate area, as shown in Figure 6.

Table 7 Design and performance of lugged wheels based on the expected level of wheel sinkage during operation

Design parameters and performance of the lugged wheel	Optimal lugged wheel design		
	Sinkage = 5 cm	Sinkage = 10 cm	Sinkage = 15 cm
Wheel diameter (cm)	77	77	77
Number of lugs (pieces)	8	8	9
Lug width (cm)	7	7	7
Lug length (cm)	28	28	28
Lug angle (°)	20	20	20
Vertical force (F_v) (kg)	138.97	155.51	291.56
Horizontal force (F_h) (kg)	152.04	170.83	350.12
Torque (Nm)	508.87	571.82	1175.14
Wheel design			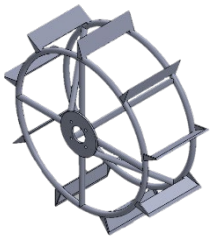

The results showed that a higher soil depth and angle of emphasis led to an increase in the penetration resistance, which is possible if the land is often passed by tractors during tillage and harvesting (Kasirajan et al., 2024; Liang et al., 2020; Linh et al., 2015). Furthermore, this data was analysed to predict soil penetration resistance at each depth and angle of plate pressure using the backpropagation neural network method, which affects the design parameters of the lug wheel (Ünal et al., 2022, 2024; Rizaldi et al., 2018). Consideration of the dynamics and kinematics of the wheel during operation also showed that several lugs were active, each having a different reaction force according to the depth and angle. Moreover, the forces acting on the wheel indicated that the lugs were required to provide thrust (F_h) and lifting (F_v) forces for the wheel to move forward. The F_h and F_v values produced by each active lug depended on the weight and methods used to apply the tractor. Therefore, tractor data were also found to be necessary in addition to the physical properties of the soil (Table 2), including the tractor weight, which significantly affected the amount of pressure the lugs exerted on the soil, as well as the wheel space to determine the maximum diameter of the wheels. These parameters differ for different types of tractors; therefore, they must be specified during the wheel design process.

The data relating to the tractor and physical properties of soil in Table 6 show that the vertical loads to be overcome by the wheel (F_v) were ≥ 136.6 kg and the horizontal loads (F_h) were ≥ 77.05 kg. This indicates that F_v and F_h produced by the lugged wheels must be larger than F_v and F_h required for the tractor to operate. The design method developed in this study was observed to produce optimal wheels for use in paddy fields based on sinkage. This was achieved by calculating the soil penetration depth during operation, considering the difference in the hardpan layers of the paddy field soil. The lugged wheel was designed for operation depths of 5, 10, and 15 cm, and the calculated optimal designs are listed in Table 7.

According to the results presented in Table 7, three designs of lugged wheels were recommended for use in the paddy field at average sink depths of 5, 10, and

15 cm. The designs for 5 and 10 cm were identical. By contrast, the design for 15-cm sinkage had different F_h, F_v, and torque values. The distance between the lugs is known to have no real effect on the produced torque (Nakanishi et al., 2020).

Understanding the interaction between wheels and soil is essential for optimising wheel design to operate under a wide range of soil conditions (Wang et al., 2023; Lv et al., 2023), and wheel design can be adapted to different soil characteristics (Jayalekshmi and Gireesh Kumar, 2019; Salazar Luces et al., 2020). A proper lug design can improve the traction performance of the wheels (Du et al., 2017).

Several important factors must be considered in the design of agricultural vehicles, particularly hand tractors. First, the weight of the tractor must be calculated to match the ground conditions over which it passes. In addition, the traction ability or towing capacity of the tractor affects how effectively it pulls loads. Furthermore, the interaction of the tractor with the soil during operation and how the soil behaves under the influence of wheel force should be determined to maintain the stability and increase the efficiency of the tractor. Therefore, the application of terramechanical principles, soil mechanics theory, and vehicle engineering is indispensable to ensure that tractors operate in an energy-efficient, economical, and environmentally friendly manner.

In addition, the strength of the soil, particularly in paddy fields, must be considered to determine whether it can support the load of a hand tractor passing over it. The pressure exerted by the tractor on the soil must be lower than the soil penetration resistance to prevent the lugged wheels of the tractor from sinking. Therefore, when determining the design parameters of tractor wheels, factors such as the wheel diameter, number of lugs, lug size, and lug angle must be considered. This is used to generate the lifting force, pulling force, and traction required by the wheels to carry the tractor and its attachments effectively. By doing so, tractors may be more easily operated in paddy fields.

Economic aspects should also considered by optimising the material requirements used to reduce wheel manufacturing costs. Consequently, the operational costs of the tractor can be minimised, and movement can be made smoother and more efficient. This has been noted in a previous study (Md-Tahir et al., 2023), wherein the relationships between the wheel parameters, soil stress, thrust characteristics, and wheel drive force were derived. It was demonstrated that the traction performance, power transfer efficiency, and trafficability of tractors operating in loose terrain can be improved by optimizing the wheel parameters.

4 Conclusion

In this study, the design parameters for a lugged wheel were determined using equations developed based on the dynamics and mechanics of the wheel movement in soil. The process focused on using the soil penetration resistance and specifications of the tractor as inputs. This led to the production of an optimal lugged-wheel design with the ability to operate at different depths. Considering the varied soil depth of the paddy fields at the research location (10–25 cm), the recommended design specified a wheel diameter of 77 cm using nine lugs with a width of 7 cm, length of 28 cm, and an angle of 20° under the assumption that the tractor wheels operate at a depth of 15 cm. The vertical force, horizontal force, and resulting torque also ensure the proper and stable operation of the tractor. The proposed design was found to be suitable only for the paddy fields considered in this study because lug-wheel design depends on the land conditions and tractor type.

References

Agarwal, S., C. Senatore, T. Zhang, M. Kingsbury, K. Lagnemma, D. I. Goldman, and K. Kamrin. 2019. Modeling of the interaction of rigid wheels with dry granular media. *Journal of Terramechanics*, 85: 1-14.

Aoshima, K., M. Servin, and E. Wadbro. 2021. Simulation-based optimization of high-performance wheel loading. arXiv preprint arXiv:2107.14615.

Bao, Y., J. Yang, Y. Zhao, X. Liu, Y. Guo, Z. Li, and J. Xiang. 2020. Design of the walking driving system for a blueberry harvester based on contact mechanical

behavior of wheel-soil. *Transactions of the Chinese Society of Agricultural Engineering*, 36(7): 43-52.

Chen, Z., J. Gu, and X. Yang. 2020. A novel rigid wheel for agricultural machinery applicable to paddy field with muddy soil. *Journal of Terramechanics*, 87: 21–27.

Delmond, J. G., W. D. S. Guimarães Junnyor, M. F. D. Brito, D. F. Rossoni, C. F. Araujo-Junior, E. D. C. Severiano, and E. C. Severiano. 2024. Which operation in mechanized sugarcane harvesting is most responsible for soil compaction? *Geoderma*, 448: 116979.

Du, Y., J. Gao, L. Jiang, and Y. Zhang. 2017. Numerical analysis of lug effects on tractive performance of off-road wheel by DEM. *Journal of the Brazilian Society of Mechanical Sciences and Engineering*, 39(6): 1977–1987.

Fajardo, A. L., and D. C. Suministrado. 2019. Effect of lug angle, forward and shaft speeds, and number of passes on puddling characteristics and performance of the tilling wheel of float-assisted tiller. *Philippine Journal of Agricultural and Biosystems Engineering*, 15(1): 3-12.

Feng, L., X. Jiang, and A. Song. 2022. An instrumented wheel-on-limb system of planetary rovers for wheel-terrain interactions: System conception and preliminary design. In *Proc. of the 2022 2nd International Conf. on Robotics and Control Engineering*, 96-101. Nanjing, China, 25-27 March.

Gao, H., R. Yuan, Z. Liu, and R. Lu. 2024. Design and analysis of a lunar crewed vehicle with a novel versatile compliant suspension mechanism. *Journal of Mechanisms and Robotics*, 16(12): 121002.

Jayalekshmi, S., and P. Gireesh Kumar. 2019. Studies on the sinkages of rigid plain wheels and lugged wheels on TRI-1 lunar soil simulant. *Journal of Terramechanics*, 82: 35–42.

Kasirajan, S., T. Parthipan, S. Elamathy, G. S. Kumar, M. Rajavel, and P. Veeramani. 2024. Dynamics of soil penetration resistance, moisture depletion pattern and crop productivity determined by mechanized cultivation and lifesaving irrigation in zero till blackgram. *Heliyon*, 10(7): e28625.

Kim, C. H., and D. I. Cho. 2023. DNN-based slip ratio estimator for lugged-wheel robot localization in rough deformable terrains. *IEEE Access*, 11: 53468–53484.

Kim, Y. S., T. J. Kim, Y. J. Kim, S. D. Lee, S. U. Park, and W. S. Kim. 2020. Development of a real-time tillage depth measurement system for agricultural tractors: Application to the effect analysis of tillage depth on draft force during plow tillage. *Sensors*, 20(3): 912.

Liang, L., X. Chen, K. Sun, R. He, X. Wang, and Q. Ding. 2020. Effects of harvester on soil disturbance in rice-wheat rotating areas in the lower reaches of Yangtze River region. *Journal of Nanjing Agricultural University*, 43(1): 186–193.

Linh, T. B., S. Sleutel, G. V Thi, K. Le Van, and W. M. Cornelis. 2015. Deeper tillage and root growth in annual rice-upland cropping systems result in improved rice yield and economic profit relative to rice monoculture. *Soil and Tillage Research*, 154: 44–52.

Lv, F., N. Li, H. Gao, L. Ding, Z. Deng, H. Yu, and Z. Liu. 2023. Vibration-based recognition of wheel–terrain interaction for terramechanics model selection and terrain parameter identification for lugged-wheel planetary rovers. *Sensors*, 23(24): 9752.

Md-Tahir, H., J. Zhang, Y. Zhou, M. Sultan, F. Ahmad, J. Du, A. Ullah, Z. Hussain, and J. Xia. 2023. Engineering design, kinematic and dynamic analysis of high lugs rigid driving wheel, a traction device for conventional agricultural wheeled tractors. *Agriculture*, 13(2): 493.

Nakanishi, R., H. Nakashima, J. Miyasaka, and K. Ohdoi. 2020. Tractive performance analysis of a lugged wheel by open-source 3D DEM software. *Journal of Terramechanics*, 92: 51–65.

Pentoś, K., and K. Pieczarka. 2017. Applying an artificial neural network approach to the analysis of tractive properties in changing soil conditions. *Soil and Tillage Research*, 165: 113–120.

Rizaldi, T., W. Hermawan, T. Mandang, S. Pertiwi, and R. Rudiyanto. 2018. Development of the method on the prediction of soil plat penetration resistance. *Scientia Agriculturae Bohemica* , 49(4): 325–332.

Rizaldi, T. and Sumono. 2020. Prediction of lugged wheels performance through soil penetration resistance measurement against pressure plate. *Internatonal Agricultural Engineering Journal*, 29(1): 1–5.

Salazar Luces, J. V., S. Matsuzaki, and Y. Hirata. 2020. RoVaLL: Design and development of a multi-terrain towed robot with variable lug-length wheels. *IEEE Robotics and Automation Letters*, 5(4): 6017–6024.

Staněk, R., T. Kerepecký, A. Novozamský, F. Šroubek, B. Zitová, and J. Flusser. 2023. Real-time wheel detection and rim classification in automotive production. In *2023 IEEE International Conference on Image Processing (ICIP)*, 1410-1414. Kuala Lumpur, Malaysia, 8-11 October.

Ünal, İ., Ö. Kabaş, S. Sözer, and S. Çetin. 2022. Prediction of soil penetration resistance with three different artificial neural networking methods. *Romanian Agricultural Research*, 36: 447-456.

Ünal, İ., Ö. Kabaş, and S. Sözer. 2024. Comparison of two different artificial neural network models for prediction of soil penetration resistance. *Journal of Agricultural Engineering*, 55(1): 1550.

Wang, Z., H. Yang, L. Ding, B. Yuan, F. Lv, H. Gao, and Z. Deng. 2020. Wheels' performance of Mars exploration rovers: Experimental study from the perspective of terramechanics and structural mechanics. *Journal of Terramechanics*, 92: 23–42.

Wang, Z., L. Ding, H. Yang, Q. Lan, H. Gao, and Z. Deng. 2023. Linear prediction of high-slip sinkage for planetary rovers' lugged-wheels based on superposition principle. *IEEE Robotics and Automation Letters*, 8(3): 1247–1254.

Yang, Y., M. Zhang, Y. Sun, N. Liu, and H. Pu. 2018. Interaction characteristics between an active lugged wheel with a single lug and sand soil. *Journal of Harbin Institute of Technology*, 50(7): 119–125.

Zhou, H., J. Zhang, Y. Zhu, C. Zhang, H. M. Tahir, and J. Xia. 2017. Design and experiment of combined tillage machine for subsoiling and rotary burying of straw incorporated into soil. *Transactions of the Chinese Society of Agricultural Engineering*, 33(22): 17–26.